Journal of Coastal Research	SI	51	195-204	West Palm Beach, Florida	Summer 2010

Wave-induced Sand re-Suspension at Dredged Gravel Pits based upon Hydrodynamic Measurements (Tromper Wiek, Baltic Sea)

Erwan Garel [1*] and Alice Lefebvre[1]**

[1] National Oceanography Centre, Southampton
European Way, Southampton
SO143ZH, United Kingdom

[*] Present address: CIACOMAR
University of Algarve
Avenida 16 de Junho
8700-311 Olhão
Portugal
egarel@ualg.pt

[**] Present address:
MARUM - Center for Marine Environmental Sciences
University of Bremen
Leobener Str.,
D-28359 Bremen, Germany

ABSTRACT

Gravel pits created by anchor hopper dredging may affect regional sediment transport patterns by trapping sediments. In turn, this may cause -or enhance- erosion at the adjacent coastline. Reliable assessment of such impacts requires a good understanding of the hydro-sediment dynamic processes acting at dredged pits. This paper examines the processes for sand re-suspension from pressure, current and turbidity data collected inside and outside a single dredged pit, in a non-tidal environment (Tromper Wiek, Baltic Sea). The data confirm the generally weak sediment dynamics in the area, with waves being the main hydrodynamic agent for sediment re-mobilization. Comparisons with historical data indicate a small number of sediment re-suspension events (<15%), over a 37 months-long period, without significant difference inside and outside the pit. Suspended sediment concentration profiles are predicted inside the studied pit by a simplistic model, tuned to over-estimate sediment re-suspension. The results suggest that the depth of the excavation should be very shallow (<1 m) for the bed material to be frequently extracted out by waves, and redistributed over the area. With pits up to 7 m-deep within the extraction zone, we conclude that a significant fraction of sediment is trapped over the long-term period (years).

ADDITIONAL INDEX WORDS: *dredging, suspended sediment concentration.*

INTRODUCTION

The volume of gravel extracted from the seabed has significantly increased since the 1980s, in response to growing demand of the market (ICES, 2001). Offshore gravel extraction is generally carried out by means of anchor suction dredging. The technique generates rounded craters on the seabed, typically 10-50 m in diameter and up to 10 m in depth. The unwanted fraction of (fine) material is screened onboard and dumped back into the sea. These operations may have negative effects upon the marine environment, including the benthic communities and sediment transport patterns (e.g. Boyd *et al.*, 2005; Kenny and Rees, 1996; Kortekaas *et al.*, this volume). Thus, in a number of countries, Environmental Impact Assessment (EIA) and Coastal Impact Studies (CIS) are required before granting licenses for extraction (Radzevičius *et al.*, this volume). With respect to sediment dynamics, dredging close to the shore may affect the coastal sediment budget by trapping fine sediments, and cause -or enhance- coastline erosion. A comprehensive understanding of the hydro- sediment dynamic processes acting at dredged pits is important to assess these harmful effects.

Recently, increasing attention has been put upon the hydrodynamic impacts and regeneration (refilling) processes of (dredged) sand trenches (e.g. the European projects PUTMOR (Boers, 2005) and SANDPIT (Van Rijn *et al.*, 2005)). These excavations present gentle internal slopes, and are surrounded by large amounts of sand. By contrast, dredged gravel pits

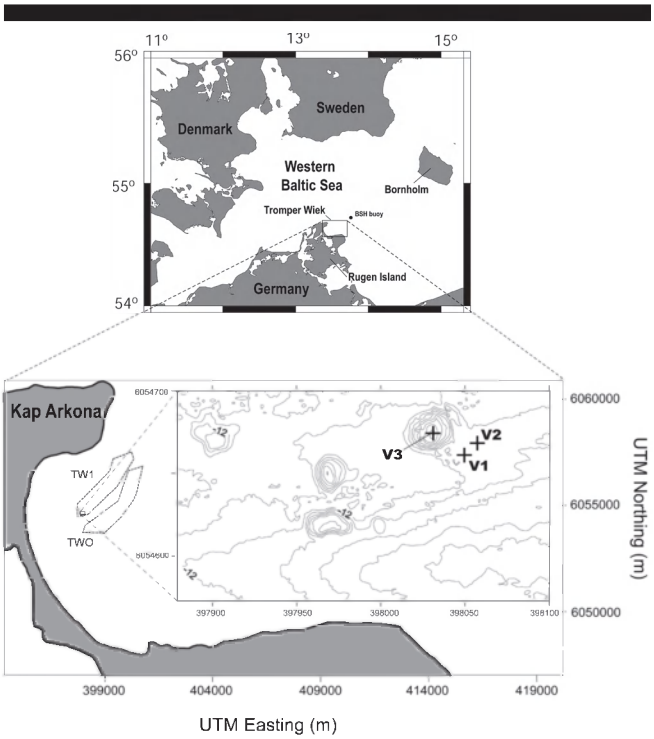

Figure 1. Location map of the studied area; insert: detail of the mooring zone (contour interval: 0.5m) with location of the ABLs. TW1: Gravel extraction site "Tromper Wiek 1"; TWO: sand extraction site "Tromper Wiek Ost".

DOI: 10.2112 / SI51-018.1 received 15 January 2007; accepted in revision 15 August 2007.

have steep walls, and sand is distributed in patches nearby the pits (due to the settling out of the fines during the screening process) (KUBICKI, MANSO, and DIESING, 2007). These differences in morphology and material availability imply distinct hydro-sediment dynamic conditions (e.g. flow structure and time-evolution) for both types of excavations.

The morphological changes and regeneration processes of dredged gravel pits have been the subject of several investigations, at the Tromper Wiek area (Baltic Sea) (Figure 1) (DIESING, 2003; DIESING *et al.*, 2006; FIGGE *et al.*, 2002; KLEIN, 2003; KUBICKI, MANSO, and DIESING, 2007; ZEILER *et al.*, 2004) However, apart from KLEIN (2003), no direct hydrodynamic measurements have been performed inside gravel dredged pits. In this paper, we present new hydrodynamic data collected in the same area, during a 4-days period which includes a storm event. Pressure, current and turbidity data, from both inside and outside a dredged gravel pit, are compared and discussed, in order to specify the processes responsible for fine material remobilization. In particular, we examine if some sand can be naturally extracted out of the pit due to the waves' action.

The organization of the paper is as follows. The first part describes the hydrodynamic and geological settings of the studied area. The next section presents the methods used to collect and process the data. In particular, a model to predict wave-induced bed shear stress is described. The results are provided in the following section. The subsequent discussion focuses on several points: firstly, we investigate the difference in suspended sediment concentration which has been observed inside and outside the studied pit; secondly, the relative number of sediment re-suspension events, over the long-term period, is characterized, based upon our records and historical data; next, we propose that sand is hardly extracted out of the pit by waves, on the basis of a simple sediment re-suspension model; additionally, we confirm that currents have no significant effect upon the upward diffusion of sand; at last, prior to conclude, we discuss the impact of dredged pits from a sediment transport perspective.

SETTING

Tromper Wiek is a semi-enclosed bay in the Western Baltic Sea, with low sediment dynamics intensity (DIESING, 2003) (Figure 1). Tidal currents are hardly discernable in this practically non-tidal environment (the tidal range is a few cm). Although wind driven currents may have some significance, the waves are the most important hydrodynamic agent for sediment mobility. The bay is located east of a spit, between two headlands, in the northern part of Rügen Island (Figure 1). Due to this coastal configuration, Tromper Wiek is exposed only to waves from the 0-90° quadrant, with a maximum fetch of about 90 km (Figure 1). Throughout the year, westerly winds dominate. High waves are only generated during the late winter and early spring (February to May), when strong easterly to northeasterly winds prevail (MOHRHOLZ, 1998).

Sand and gravel extraction has been carried out at Tromper Wiek for many years (Figure 1). Within the gravel extraction site (Tromper Wiek 1), between 9 and 16 m water depth, the seafloor is marked with craters 5 to 50 m in diameter and up to 7 m-deep. These features have proved to be stable for several years, at least (FIGGE *et al.*, 2002). In detail, spatial extension of the edge of the pits is observed over the years, due to collapsing of the walls (KUBICKI, MANSO, DIESING, 2007). It is estimated that among the 460,000 m^3 of sediment extracted between 1988 and 2000, half of this volume was dumped back into the sea (BRAUCKHOFF, cited in DIESING *et al.*, 2006). Thus, patches of fine sediment (<2 mm in diameter, mostly sand) are commonly found in the vicinity of the pits (DIESING, 2003). These deposits constitute a possible source of pit refilling. In agreement, core analyses demonstrate the episodic occurrence of sand advection inside the craters (DIESING, 2003; MANSO *et al.*, this volume), and repeated side-scan sonar surveys show the presence of bedforms together with rapid changes in the pattern of the sand patches (DIESING, 2003; DIESING *et al.*, 2006). Based upon acoustic seafloor imaging, KUBICKI, MANSO, and DIESING (2007) observed a decrease in the availability of sand around a pit and a deceleration of the mean (pit) refilling rate, over a 6 years period. The key mechanisms for sediment remobilization are the near-bed orbital motions induced by surface waves entering the bay (KLEIN, 2003).

METHODS

Data acquisition

Hydrodynamic data were acquired using three self-recording Autonomous Benthic Landers (ABLs), from the 19th to the 23rd of October 2004. Each ABL consists of a device (VALEPORT 808) mounted on a frame weighted with chains. The devices are fitted with a pressure gauge, an Electro-Magnetic Current-Meter (EMCM) and an Optical Backscatter Sensor (OBS). The EMCM and OBS measure the northward and eastward components of the flow (in a horizontal plan), and the scattering of infrared radiation by suspended particles, respectively. One ABL (referred as V3, hereafter) was deployed at ~14.5 m water depth, inside a circular dredged pit (at 54.6291° N; 13.4208° E). The selected pit has been investigated previously by KLEIN (2003) and KUBICKI, MANSO, and DIESING (2007). From multibeam bathymetry, the excavation was, in December 2003, 3.5 m-deep and ~30 m in diameter (KUBICKI, MANSO,and DIESING, 2007). The two other ABLs (referred as V1 and V2, hereafter) were moored at about 20 m from the edge of the pit, at ~11 m water depth (Figure 1). Scuba-divers checked the location of the moorings, within sandy patches displaying symmetrical ripples.

The ABLs were set up to record the pressure, horizontal currents and turbidity at 4 Hz, during bursts of 8 min 32 sec, every 30 min. The pressure sensor, OBS and EMCM were at 0.5, 0.45 and 0.25 m above the sea bed, respectively. In addition, a 20 cm-high cylinder, opened at top, was attached vertically to the frames, in order to trap sediments at the height of the OBS. These traps were collected by scuba-divers at the end of the experiments, together with bed sediment sampled nearby the instruments.

The ABLs were triggered at the same time, allowing direct comparison of the burst records. Because stations V1 and V2 were located relatively close to each others, their outputs are very similar; only the results of station V1 are presented here and compared to the data collected inside the pit (V3).

One hour-averaged wind and air pressure data from Kap Arkona meteorological station (see Figure 1 for location) were provided by the German Weather Forecast Agency. In addition, historical wave parameters were obtained from the BSH (Federal Maritime and Hydrographic Agency); the dataset consists of the readings (significant wave heights, direction, period and wavelength) from a buoy located in the entrance to the bay (Figure 1), between 2003 and 2006, at a 30 min time interval.

Data processing

The pressure is converted to sea surface elevation with standard calculations methods assuming linear wave theory, as described by TUCKER and PITT (2001). A frequency-dependent pressure correction factor that compensates for depth attenuation is applied to wave frequencies from 0.05 to 0.33 Hz. The significant wave height (Hs) and peak period (Tp) are derived from spectral analysis applied to each burst.

Three techniques were combined for grain size analysis: Coulter counter for the mud fraction; settling tower for the sand fraction; and, sieving for coarser grained sediments. The statistics of the particle size distribution are described according to MCMANUS (1988). The distribution of the bottom sediment should be considered with caution. The divers reported the loss of some fines during the sampling, and it is suspected that the d_{50} of the bed sediment is slightly finer than proposed. In addition, sediment distributions are highly variable, even at nearby locations, in relation with the heterogeneous nature of the seafloor (DIESING, 2003).

The observed turbidity was converted to suspended sediment concentration (SSC) in laboratory. Various known concentrations of sediment were stirred in a bucket, during OBS measurements, and a regression was applied to the resulting concentration-turbidity graph. The calibration was performed with the sediments from the traps, i.e. which were in suspension at the height of the sensor during the experiment. The following polynomial equation yields the best correlation coefficient (0.82), and was therefore used to convert the turbidity (T, in Volts) into suspended sediment concentration (SSC, in mg/l) (Figure 2):

$$SSC = 110.36T^2+16.275T \quad (1)$$

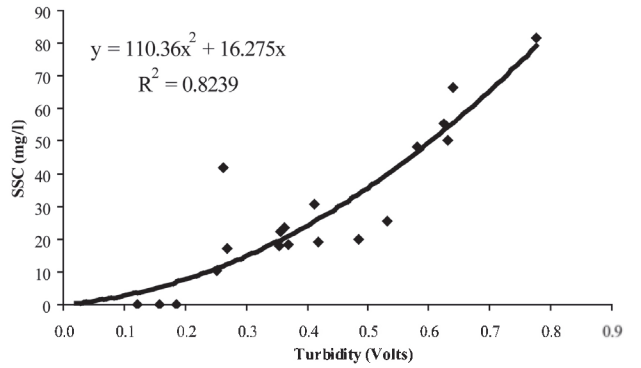

Figure 2. Calibration curve of the OBS.

Bed shear stress

Due to the weakness of the flow during the experiment, the bed shear stress results essentially from the activity of the waves. The wave induced bed shear stress is computed from the near-bed significant orbital velocity (U_{ws}), using SWART (1974) friction factor (F_w) for rough turbulent flow:

$$\tau_w = 0.5\rho F_w U_{ws}^2 \quad (2)$$

with

$$F_w = 0.00251\exp(5.21r^{-0.19}) \quad (3)$$

where r is the relative roughness:

$$r = A/K_s \quad (4)$$

with K_s, the Nikuradse roughness. The grain related bed shear stress is computed using:

$$K_s = 2.5d_{50} \quad (5)$$

where d_{50} is the median grain diameter of the bed material. To compute the total bed shear stress, the Nikuradse roughness (K_s) is derived from the total bed roughness (Z_o) through the relationship:

$$K_s = 30Z_o \quad (6)$$

Z_o is the sum of the skin friction component ($d_{50}/12$) and form drag component of the bed roughness (Z_{of}). Following NIELSEN (1992), Z_{of} is obtained from the wave ripples height (H_r) and wavelength (L_r):

$$Z_{of} = 0.267H_r^2/L_r \quad (7)$$

where the size of the ripples is estimated for mobile sand, based upon the wave mobility number (Ψ) and the skin friction Shields parameter (θ_s):

$$H_r = A(0.275-0.022\Psi^{0.5}) \quad (8)$$

$$L_r = H_r/(0.182-0.24\ \theta_s^{1.5}) \quad (9)$$

Ψ and θ_s are defined by:

$$\Psi = U_{ws}^2/[gd_{50}(s-1)] \quad (10)$$

$$\theta_s = \tau_{ws}/[gd_{50}(\rho_s - \rho)] \quad (11)$$

with g, the acceleration due to gravity (9.81 m/s^2), τ_{ws}, the skin friction bed shear stress, ρ_s, the sediment density (2650 kg/m^3), ρ, the water density (1027 kg/m^3), and s, the ratio of grain and water densities (ρ_s/ρ). It has been verified that the wash-out conditions (Ψ=156 and θ_s=0.831) were not met during the period of measurements.

In equations (4) and (8), A is the wave semi-orbital excursion:

$$A = U_{ws}T_p/(2\pi) \quad (12)$$

The significant orbital velocity is considered as more representative of the waves' activity than the maximum orbital velocity, during a burst. The orbital velocities are computed for each burst from the EMCM records. The latter are filtered to eliminate the velocity components not related to waves (high pass, 0.1 Hz cut off frequency). The filtered velocity components are rotated in the direction of the waves, and analyzed in the spectral domain, to yield the significant (crest and trough) near-bed wave orbital velocities (i.e. above the wave boundary layer). The difference between the crest and the trough values is generally less than 0.2 cm/s, with a maximum of about 1 cm/s, observed at V1 during the storm, for corresponding significant orbital velocities about 25 cm/s. Thus, the waves can be reasonably considered as symmetrical. Only the crest orbital velocities were used for calculations.

The bed is mobile when the maximum grain related bed shear stress is higher than the critical bed shear stress (τ_{cr}), derived from equation (11), where θ_{cr}, the threshold Shields parameter is obtained using SOULSBY'S (1997) formula:

$$\theta_{cr} = 0.30/(1+1.2D) + 0.055[1-\exp(-0.02D)] \quad (13)$$

where D is the dimensionless grain-size:

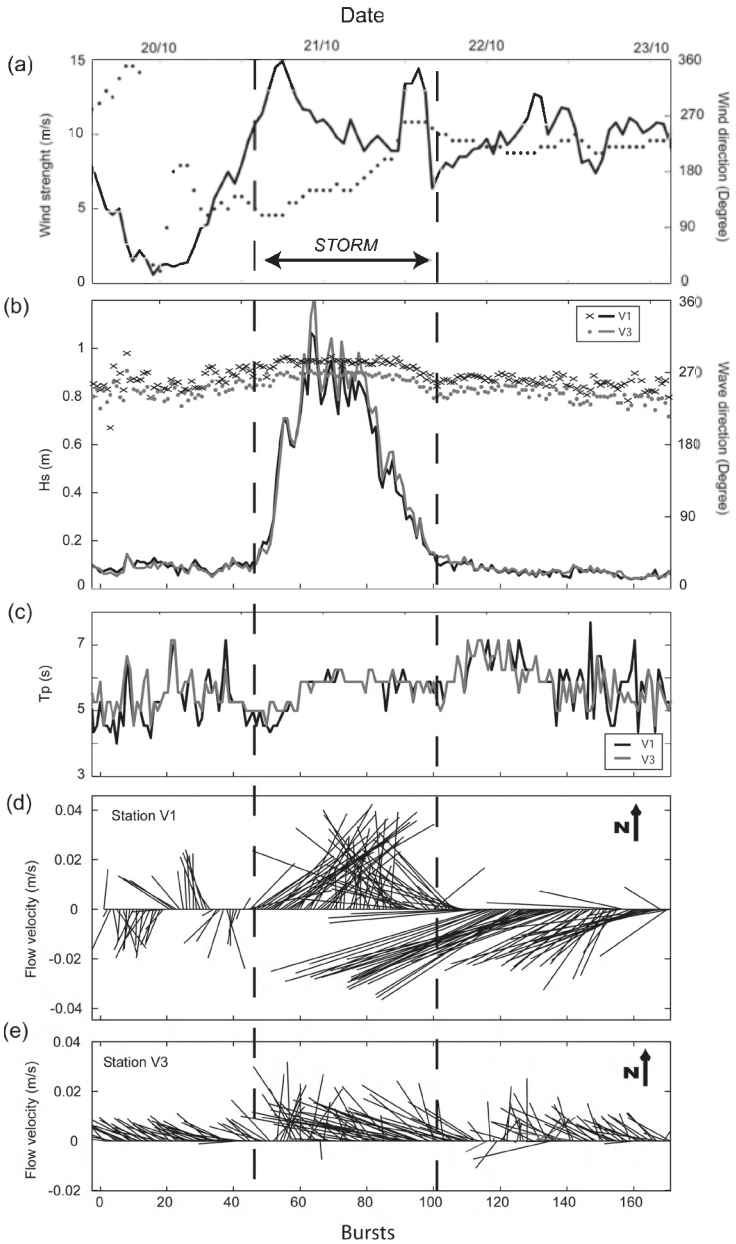

Figure 3. Wind and hydrodynamic conditions during the experiment; (a) wind strength (line) and direction (reported from which it originates, with dots); (b) significant wave height (line) and direction of advance (marks) at both stations (V1: black line and crosses; V3: grey line and dots); (c) Wave peak period at both stations (V1: black; V3: grey); (d) stick plot of the averaged currents at station V1; e) stick plot of the averaged currents at station V3.

Table 1. *Statistical grain-size parameters and descriptive terms after McMANUS (1988).*

Sample	d_{50}	Classification	Sorting	Skewness	Kurtosis
V1 bed	0.5mm	coarse/medium sand	moderately sorted (0.84)	positively skewed (0.08)	leptokurtic (1.2)
V3 bed	0.34mm	medium sand	well-sorted (0.46)	Symmetrical (-0.03)	mesokurtic (0.98)
V1 trap	0.1mm	very fine sand	poorly sorted (1.21)	symmetrical (-0.07)	leptokurtic (1.19)
V3 trap	0.07mm	very fine sand	poorly sorted (1.43)	symmetrical (-0.09)	leptokurtic (1.24)

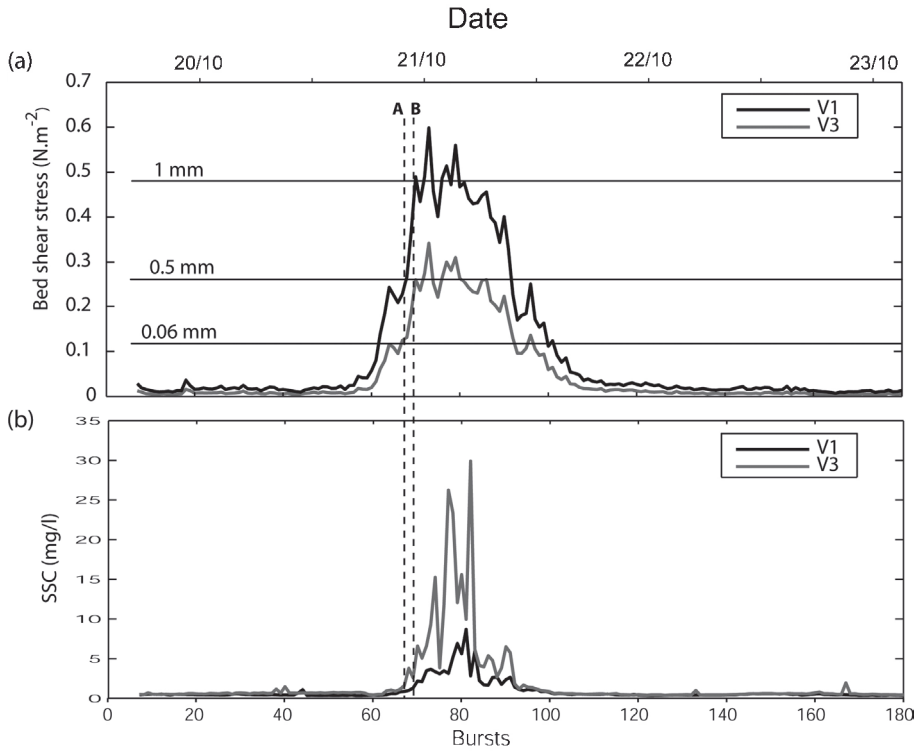

Figure 4. (a) bed shear stress at V1 (black) and V3 (grey), and threshold of motion for grain-sizes of 0.06, 0.5 and 0.1 mm; (b) observed SSC (mg/l). Lines A and B indicate the beginning of the SSC peak at V3 and V1, respectively.

$$D = d_{50}\,[g(s\text{-}1)/\upsilon^2]^{1/3} \quad (14)$$

with υ, the kinematic viscosity ($1.36.10^{-6}$ m²/s).

RESULTS

From the morning of October 20th, an easterly to south-easterly wind was recorded at Kap Arkona, with an increasing strength peaking at 15 m/s in the afternoon (Figure 3a). Stormy waves, with a saw-toothed significant height signal, up to 1.2 m, were generated inside the bay (Figure 3b). About midday of October 21st, a still strong (about 10 ms/) southwesterly to westerly wind sets in, until the end of the deployment period. The change in wind direction induced a rapid decrease in wave activity, due to the sheltering effect of the coast. During the 26 hours-long storm, the peak period remained fairly constant, about 6 sec, typical of locally generated waves (Figure 3c). The waves were directed towards the west during the whole experiment (Figure 3b). In agreement, coincident side-scan sonar records displayed symmetrical ripples, with ~N-S crest orientation, over the sandy patches and inside the pits (Manso *et al.*, this volume). A systematic slight angle between the wave direction at stations V1 and V3 can be observed. This is attributed to refraction due to changes in bathymetry nearby the pit.

The currents present significant differences inside and outside the pit. At the outer station V1, the flow is about 2, 5 and up to 8 cm/s before, during and after the storm, respectively (Figure 3d). The direction of the flow shows no relation to the waves and wind, suggesting a complicated pattern of water circulation in the bay (this circulation is probably induced mainly by the wind, which pushes the water in or out of the bay). The flow is towards the NE at the beginning of the storm, and then rotates anticlockwise, to the SW, after the storm (Figure 3d). In contrast, the flow recorded at station V3, inside the pit, is weaker, with peak velocities up to 3 cm/s, during the storm (Figure 3e). Apart from short periods of time, its direction is almost constantly towards the NW. This indicates a decoupling of the flow inside and outside the pit, as previously observed by Klein (2003). Nevertheless, the flow orientations inside and outside the pit are better correlated during the storm. Thus, the pit hydrodynamics appears to relate as well to the wind-driven water circulation in the bay during extended periods of strong easterly winds.

The statistical grain-size parameters of the sediment sampled near the ABLs and collected in the traps are displayed in Table 1. Bed sediments are finer (d_{50}=0.34 mm) and better sorted inside the pit (V3), compared to station V1 (d_{50}= 0.5mm). The sediments in the traps consist of poorly-sorted fine sand, with d_{50}=0.1 and 0.07 mm at stations V1 and V3, respectively. In addition, much more sediments were found in the trap attached to V3 (80% of the relative percentage, in weight).

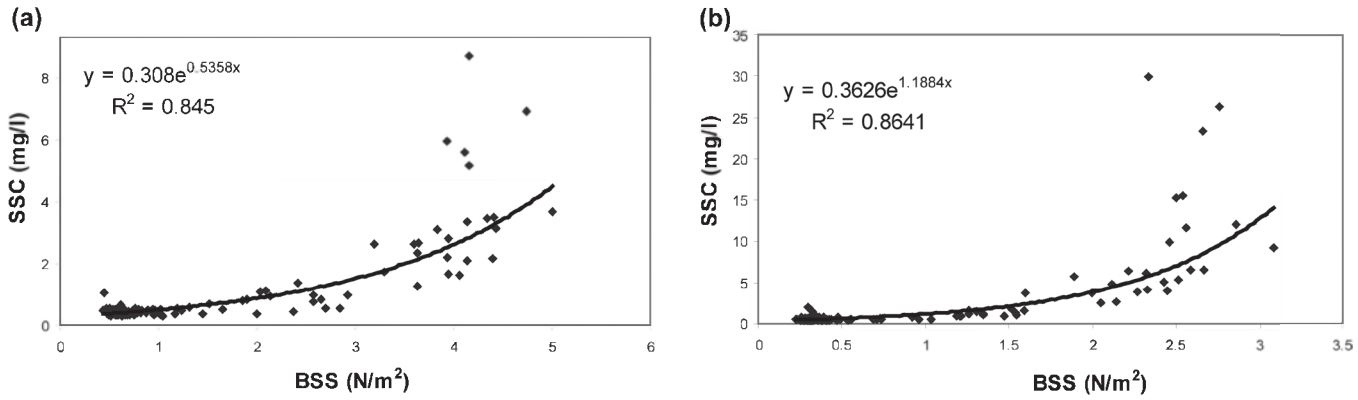

Figure 5. Predicted bed shear stress versus observed SSC, at stations V1 (a) and V3 (b).

During the storm, the predicted (grain related) bed shear stress exceeds the threshold of motion for grain-size up to 1 mm at station V1, and up to 0.5 mm at station V3 (Figure 4a). These grain-sizes correspond to 85% and 90% in weight of the entire grain-size distribution, at V1 and V3, respectively. Thus, most of the sand fraction was mobile at the studied sites during the storm. Peaks in the SSC signal are observed at V1 and V3, from a similar background value, simultaneously with the increase in bed shear stress (Figure 4b). Higher maximum concentrations were noticed inside the pit (~30 mg/l) than outside (~8 mg/l), despite a higher predicted bed shear stress at the outer station. In addition, the SSC inside the pit started to raise for a bed shear stress of ~0.12 $N.m^{-2}$, i.e. just after the threshold of motion for very fine sand (0.06 mm) was reached (Figure 4). By contrast, at V1, the SSC peak started half an hour later, for bed shear stress values about 4 times larger (~0.4 $N.m^{-2}$), when a much larger fraction of sediments was already remobilized. Relatively good correlations are observed between bed shear stress and SSC (Figure 5), with best fit lines which follow exponential law equations. However, large discrepancies are observed for high values (of the bed shear stress and SSC), i.e. during the storm.

DISCUSSION

OBS measurements are highly influenced by both the number of particles and the particle size (Xu, 1997). Thus, the differences in SSC values, observed at V1 and V3 during the storm (Figure 4b), can be explained by the presence of finer bed sediment inside than outside the pit, rather than advection from the surroundings. The presence of finer median grain diameter of the bed and trapped material at V3, compared with V1, supports this view (Table 1.); likewise, the relative volume of sediment collected inside the traps was greater inside the pit. In agreement, the SSC at V3 started to increase while the threshold of motion for very fine sand is exceeded (Figure 4). Although at a greater depth, the fines at the bottom of the pit require a relatively lower bed shear stress in order to be uplifted. In turn, they are more easily maintained in suspension, due to slower settling velocities. As an example, the settling velocity (W_s) of the sediment found in the traps (referred hereafter with the subscript 's') are determined using Soulsby's (1997) equation for natural sand:

$$W_s = (\upsilon / d_{50s})[(10.36^2 + 1.049D_s^3)^{0.5} - 10.36] \quad (15)$$

The resulting settling velocity is twice as fast at V1 (5.6 mm/s) than at V3 (2.8 mm/s). Approximately, sediment is suspended when the settling velocity is slower than the skin friction velocity (U_{*s}), the latter being function of the square root of the bed shear stress:

$$U_{*s} = (\tau_{ws} / \rho)^{0.5} \quad (16)$$

Thus, in our example, the trapped sediments at V3 require a much smaller (~4 times) bed shear stress than at V1 to remain in suspension. However, previous investigations in the area indicate that the fines inside the pit originate from the surrounding sandy patches, which material is remobilized during storms (Kubicki, Manso and Diesing, 2007; Diesing, 2003). Sediment advection might contribute partly to the SSC signal observed inside the pit during the storm.

Table 2. *Waves parameters used to predict suspended sediment concentration profiles.*

Storm	Date	Hs (m)	Tz (seconds)	Uws (m/s)	As (m)	Hrs (cm)	Lrs (cm)	Origin of the data
Mild	20/10/2004	1.3	5.4	0.19* (measured=0.2)	0.17*	3.3*	18*	This study
Severe	20/03/2001	3.1	6	0.59*	0.57*	7*(1)	40*(1)	Klein (2003)
Extreme	13/02/2005	4.3	6.7	1*	1.07*	12*	85(2)	BSH+

(*) predicted values (measured otherwise); (1) for d=0.34mm; (2) from side-scan sonar imagery; (+) period 2003-2006, 0-90° quadrant.

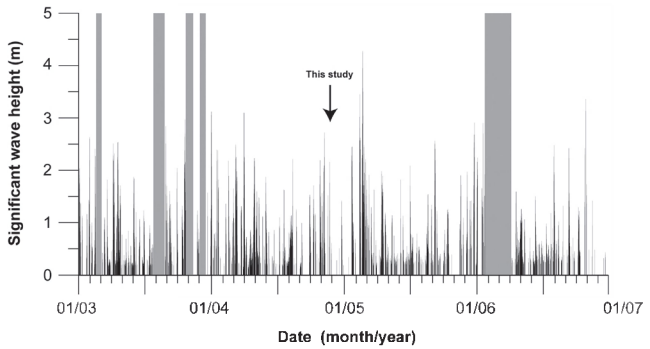

Figure 6. Significant wave heights from the 0-90o quadrant in Tromper Wiek; the periods without records are indicated in grey.

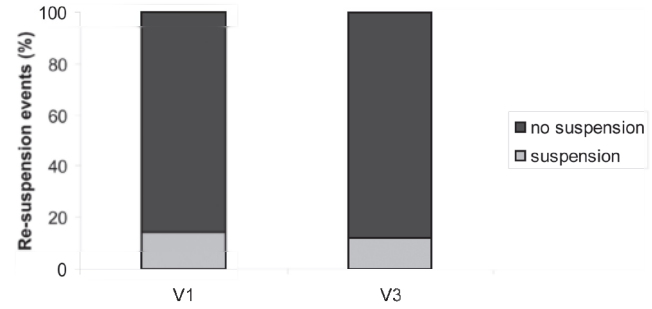

Figure 7. Percentage of sediment re-suspension events at stations V1 and V3, between 2003 and 2006; explanations in the text.

Based upon the relation between predicted bed shear stress and SSC (Figure 5), the historical waves were used to quantify the relative number of sediment re-suspension events, during the years 2003 to 2006. Due to some periods without data, the entire original dataset represents ~37 months-long (30min-averaged) continuous records. Only the waves from the 0-90° quadrant were considered, to account for the sheltering effect of the coast. The significant wave heights are presented in Figure 6.

As mentioned previously, storm events predominate between February and May (note the extreme storm which occurred in February 2005 (Hs>4 m) and the data gap during winter 2006). The bed shear stress has been predicted, based upon the model described previously, and compared to the threshold for sediment re-suspension observed inside and outside the pit (0.12 $N.m^{-2}$ and 0.4 $N.m^{-2}$, respectively) (see Figure 4). This approach documents the percentage of (wave induced) sediment re-suspension events, at 0.45 m above the bed (i.e. height of the sensor), during the 37 months-long period. Results show negligible differences inside and outside the pit (Figure 7).

Sediment re-suspension is predicted to take place during 14.3% and 12.4% of the time, at V1 and V3, respectively. These values represent less than 5.3 months of the (37 months-long) period, confirming the low intensity of the hydrodynamic activity inside the bay. Bed sediment are relatively rarely re-suspended by waves. A slow refilling of the dredged gravel pits is predicted. Towards the assessment of pits' recovery rate, it would be of interest to quantify the concentration of re-suspended sediments. This has not been done here, due to the poor relation obtained between high values of bed shear stress and SSC (Figure 5).

From the echo intensity of ADCP records, KLEIN (2003) proposed that waves may re-suspend bed sediment above the rim of the pits, allowing some material to be episodically removed and redistributed over the shallower surroundings. To test this scenario, vertical concentration profiles were computed, inside the crater (i.e. at 14.5 m water depth) for various wave

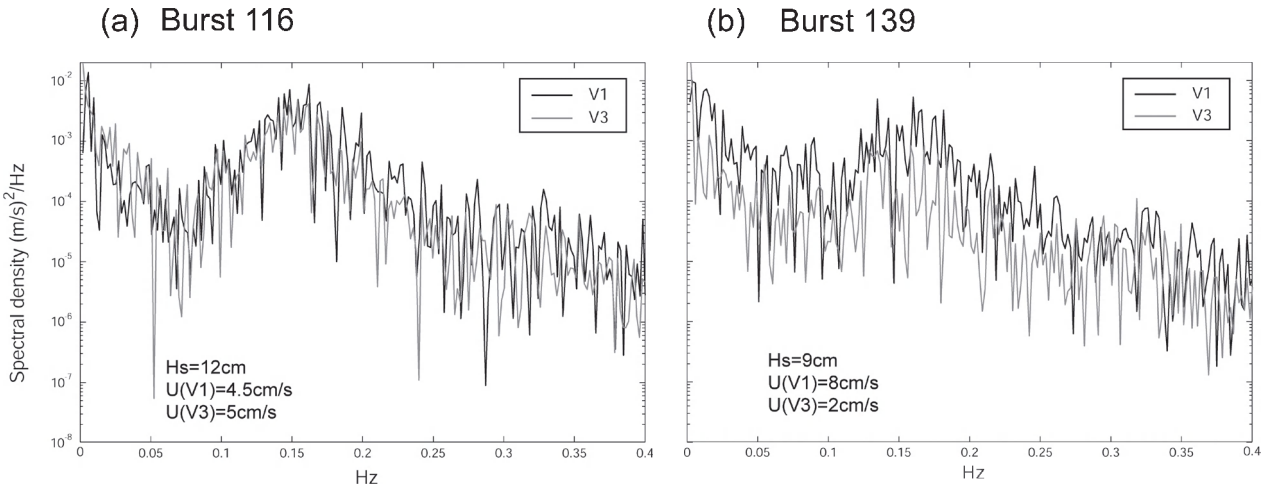

Figure 9. Semi-log plot of the flow magnitude spectrum for bursts 116 (a) and 139 (b).

conditions, referred to mild, severe and extreme storm, hereafter (see Table 2.).

For weak currents (<0.1 m/s), the SSC profile induced by waves only is similar to the one induced by combined waves and currents (VAN RIJN, 1993). Thus, only the time-average wave-induced SSC over rippled beds was modeled, using NIELSEN'S (1992) equation:

$$C(z) = C_o e^{-Z/l} \quad (17)$$

Since $U_{ws}/W_s > 18$, the vertical scale (l) corresponds to:

$$l = 1.4H_r \quad (18)$$

The reference concentration (C_o=0.005θ_r^3) is obtained from the modified effective Shields parameter (θ_r):

$$\theta_r = (F_w U_{ws}^2)/[2(s-1)gd_{50}(1-\pi H_r/L_r)^2] \quad (19)$$

The significant wave orbital velocity, U_{ws}, is estimated from:

$$U_{ws} = \pi H_s/[T_p \sinh(kh)] \quad (20)$$

where sinh is the hyperbolic sine, h, the water depth, k, the wave number (2π/L), and L, the wavelength. Comparisons show very little differences between the wave orbital velocities measured in the present study, and the ones derived from equation (19) (see mild storm, in Table 2.). Equation (17) applies to uniform bed material. For graded bottom sediment, such in the present study, the median grain diameter of the sediment in suspension will be appreciably finer than the one at the bed. In this case, as noted by SOULSBY (1997), reliable methods of predicting sediment concentration profiles under waves are not available yet. In the present model, the situation was simplified by considering a uniform bed, where the median grain diameter relates to the sediment trapped at V3 (i.e. 0.07 mm), rather than to the bed material. The objective is to test a favored case for sediment re-suspension, rather than to aim at accurate predictions. Since the suspended sediment concentration profile is very sensitive to the grain settling velocity, the model predictions are enhanced in comparison with those based upon the bed material. Likewise, ripples have been imposed to the model, to enhance the upwards sediment diffusion: for mild and severe storms, the ripple dimension has been predicted using equations (8) and (9); for extreme storms, it corresponds to large bedforms, as observed with side-scan sonar (MANSO *et al.*, this volume) (although sheet flow conditions are easily met during severe storms, for such fine sediment). The Nielsen's calibration constant (0.005) seems appropriate to compute the reference concentration (C_o), since it is derived from measurements over rippled beds and sheet flow conditions, with sand diameters between 0.08 and 0.55 mm, and wave periods between 1.0 and 9.1 sec (NIELSEN, 1986). The model fails to re-suspended material above the rim of the crater, under these optimized conditions (Figure 8). Then, it is unlikely that the bed sediment inside the pit is extracted due to the action of the waves alone, even during extreme storm events. If some sand is naturally extracted out of this pit, another process has to be considered.

Flow separation and reversal in the near-bed layer, due to adverse pressure gradients, is observed for pits with slopes of 1:5, or steeper (ALFRINK and VAN RIJN, 1983). This effect generates additional turbulence energy which may considerably reduce the settling process, and therefore, enhance the concentration of suspended material. With computed slopes of about 1:3, flow separation may take place in the studied pit. The spectral density of the flow magnitude was computed for bursts corresponding to the fastest flow and lower wave activity during the experiment, at V1 and V3 (i.e. for bursts when flow separation is expected to be the most pronounced). In the case of significant flow separation inside the pit, the flow magnitude spectra at V3 should comprise additional (high frequency) energy in comparison with V1. The results show energy peaks which correspond to the sea wave frequencies, but no significant difference is observed between V1 and V3 (Figure 9). Obviously, the current recorded during our survey were too weak to be significantly affected by the morphology (~3 cm/s, at maximum, inside the pit). The fastest currents measured by KLEIN (2003) at the bottom of the pit, in March and April 2001, were less than 8 cm/s (and only ~4 cm/s during the severe storm of March 2001). Based upon these observations, storms are not associated with stronger bottom currents. Thus, flow separation has probably a reduced effect, if any, on the suspended sediment concentration profile in the dredged pits.

Dredged pits have minimal impacts upon (regional) sediment transport patterns if their bottom (fine) sediments are frequently extracted by waves' action. At a yearly scale, extreme stormy waves are too rare in the bay for frequent redistribution of these fines over the area. During the more common severe storms, significant amount of (very fine) sand are uplifted at ~1 m above a bottom lying at 14.5 m water depth (Figure 8). In other words, the model predicts frequent material removal out of ~1 m-deep pits, or less, at ~13.5 m water depth. As pointed out before, the predicted SSC profiles correspond to optimal conditions, and are therefore over-estimated. Thus, bed sediments are probably long-termed (years) trapped in pits more than 1 m-deep, with bottom at 14.5 m water depth. At this water depth, the maximum depth of excavation, for frequent wave-induced sediment extraction, is very shallow, estimated less than 1 m.

CONCLUSION

Hydrodynamic measurements were carried out at Tromper Wiek, close to the bottom of a 3.5 m-deep dredged gravel pit (14.5 m water depth), and at a shallower nearby patch of sand (11 m water depth). Our investigations confirm the generally weak sediment dynamics, governed by the waves' activity. It is estimated that sediment re-suspension events are observed, at 0.45 m above the bed, during ~5 months over a 37 months-long period (i.e. less than 15% of the time), without significant difference inside and outside the pit. During a moderate storm (Hs up to 1.2 m), most of the sand fraction was remobilized, including inside the pit. There, bed sediments are finer than at the surroundings sandy patches. They are therefore easier to uplift, resulting in relatively stronger SSC. However, it is unlikely that these fines are re-suspended high enough to be removed out of the pit, even during historical extreme storm events (Hs=5.1 m). We suggest that pits at 13-14 m water depth should be very shallow (<1 m-deep) for the fines to be frequently redistributed over the area. Dredged pits are generally much deeper (e.g. MANSO *et al.*, this volume). Thus, fine sediments located in dredged pits at 14.5 m water depth, or deeper, are probably trapped over the long-term (years).

The estimation of reliable (dredged pits) recovery rate is fundamental to carry out comprehensive environmental im-

pact assessments. Towards this objective, numerical models must be calibrated by field observations, in order to quantify accurately sediment re-suspension events under various wave conditions. For further studies, detailed investigations of the suspended sediment composition and concentration, inside dredged pits, are recommended.

ACKNOWLEDGMENTS

This work was undertaken as part of the EUMARSAND Research Training Network (European Sand and Gravel Resources: Evaluation and Environmental Impact of Extraction, HPRN-CT-2002-00222). The help of the officers and crew of the research vessel R/V *Alkor* in collecting the data is gratefully acknowledged. Thanks are extended to the German Weather Forecast Agency and BSH (Federal Maritime and Hydrographic Agency) for providing meteorological and wave data. The helpful comments of the reviewers are gratefully acknowledged.

LITERATURE CITED

Alfrink, B.J. and Van Rijn, L.C., 1983. Two-equation turbulence model for flow in trenches. *Journal of Hydraulics Division*, ASCE, 109(3), 941-957.

Boers, M., 2005. Effects of a deep sand extraction pit. *Final report of the PUTMOR measurements at the Lowered Dump Site*, Ministerie van Verkeer en Waterstaat, 87p.

Boyd, S.E.; Limpenny, D.S.; Rees, H.L., and Cooper, K.M., 2005. The effects of marine sand and gravel extraction on the macrobenthos at a commercial dredging site (results 6 years post-dredging). *ICES Journal of Marine Science*, 62, 145-162.

Diesing, M., 2003. Die Regeneration von Materialentnahmestellen in der südwestlichen Ostsee unter besonderer Berücksichtigung der rezenten Sedimentdynamik. Christian-Albrechts-Universität zu Kiel, Ph.D. thesis, 158 p. (http://e-diss.uni-kiel.de/diss_755/)

Diesing, M.; Schwarzer, K.; Zeiler, M., and Klein, H., 2006. Comparison of marine sediment extraction sites by means of shoreface zonation. *Journal of Coastal Research*, Special Issue, 39, 783-788.

Figge, K.; Zeiler, M.; Griewatsch, K.; Mittelstaedt, E.; Klein, H.; Schwarzer, K., and Diesing, M., 2002. KFKI-Projekt Regenerierung von Materialentnahmestellen in Nord-und Ostee. *Final Report, Bundesamt für Seeschiffahrt und Hydrographie*, 94p.

ICES, 2001. *Effects of extraction of marine sediments on the marine ecosystem*. WG-EXT. Copenhagen, International Council for the Exploration of the Sea (ICES), 247, 80p.

Kenny, A.J. and Rees, H.L., 1996. The effects of marine gravel extraction on the macrobenthos: results 2 years post-dredging. *Marine Pollution Bulletin,* 32(8/9), 615-622.

Klein, H., 2003. Investigating sediment re-mobilisation due to wave action by means of ADCP echo intensity data. Field data from the Tromper Wiek, western Baltic Sea. *Estuarine, Coastal and Shelf Science*, 58, 467-474.

Kortekaas, S.; Bagdanaviciute, I.; Gyssels, P.; Alonso Huerta, J.M., and Héquette, A., this volume. Assessment of the effects of marine aggregate extraction on the coastline: an example from the German Baltic Sea coast. *Journal of Coastal Research*.

Kubicki, A.; Manso, F., and Diesing, M., 2007. Morphological evolution of gravel and sand extraction pits, Tromper Wiek, Baltic Sea. *Estuarine, Coastal and Shelf Science*, 71, 647-656.

Manso, F.; Radzevičius, R.; Blažauskas, N.; Balay, A., and Schwarzer, K., this volume. Nearshore dredging on the Baltic Sea: sate after cessation of activities and regeneration assessment. *Journal of Coastal Research*.

McManus, J., 1988. Grain size determination and interpretation. *In*: Tucker, M. (ed.), *Techniques in Sedimentology*. Oxford, England: Blackwell Scientific Publications, pp. 63-85.

Mohrholz, V., 1998. Transport and mixing processes in the Pomeranian Bight. *Marine Science Reports*, 33, 106 p. (in German).

Nielsen, P., 1986. Suspended sediment concentrations under waves. *Coastal Engineering*, 10, 23-31.

Nielsen, P., 1992. Coastal bottom boundary layers and sediment transport. *Advanced Series on Ocean Engineering,* Vol. 4, Ed. World Scientific, 324 p.

Radzevičius, R.; Velegrakis, A.F.; Bonne, W.; Kortekaas, S.; Garel, E.; Blažauskas, N., and Asariotis, R., this volume. Marine aggregate extraction: regulation and management in EU member states. *Journal of Coastal Research*.

Soulsby, R L., 1997. *Dynamics of Marine Sands*. London: Thomas Telford Publications, 249 p.

Swart, D.H., 1974. Offshore sediment transport and equilibrium beach profiles. Delft Hydraulics Lab., Publ. 131p.

Tucker, M.J. and Pitt, E.G., 2001. *Waves in ocean engineering*. Elsevier, Amsterdam: Elsevier ocean engineering book series vol. 5, 521 p.

Van Rijn, L. C., 1993. Principles of sediment transport in rivers, estuaries and coastal seas. Amsterdam: Aqua Publications, 614 p.

Van Rijn, L. C.; Soulsby, R.L.; Hoekstra, P., and Davies, A.G. (eds.)., 2005. *SANDPIT, Sand Transport and Morphology of Offshore Mining Pits*. The Netherlands: Aqua Publications, 716 p.

Xu, J.P., 1997. Converting near-bottom OBS measurements into suspended sediment concentrations. *Geo-Marine Letters*, 17, 154-161.

Zeiler, M.; Figge, K.; Griewatsch, K.; Diesing, M., and Schwarzer, K., 2004. Regenerierung von materialentnahmestellen in Nord- und Ostsee. *Die Kueste*, 68, 67-98.